Interaction of Intracellular Ion Buffering with Transmembrane-coupled Ion Transport

RICHARD P. KLINE, LEONARD ZABLOW, and IRA S. COHEN

From the Department of Pharmacology, Columbia College of Physicians and Surgeons, New York, New York, 10032; and Department of Physiology and Biophysics, State University of New York, Stony Brook, New York 11794

ABSTRACT The role of the Na/Ca exchanger in the control of cellular excitability and tension development is a subject of current interest in cardiac physiology. It has been suggested that this coupled transporter is responsible for rapid changes in intracellular calcium activity during single beats, generation of plateau currents, which control action potential duration, and control of intracellular sodium during Na/K pump suppression, which may occur during terminal states of ischemia. The actual behavior of this exchanger is likely to be complex for several reasons. First, the exchanger transports two ionic species and thus its instantaneous flux rate depends on both intracellular sodium and calcium activity. Secondly, the alteration in intracellular calcium activity, which is caused by a given transmembrane calcium flux, and which controls the subsequent exchanger rate, is a complex function of available intracellular calcium buffering. The buffers convert the ongoing transmembrane calcium fluxes into changes in activity that are a small and variable fraction of the change in total calcium concentration. Using a number of simple assumptions, we model changes in intracellular calcium and sodium concentration under the influence of Na/Ca exchange, Na/K ATPase and Ca-ATPase pumps, and passive sodium and calcium currents during periods of suppression and reactivation of the Na/K ATPase pump. The goal is to see whether and to what extent general notions of the role of the Na/Ca exchanger used in planning and interpreting experimental studies are consistent with its function as derived from current mechanistic assumptions about the exchanger. We find, for example, that based on even very high estimates of intracellular calcium buffering, it is unlikely that Na/Ca exchange alone can control intracellular sodium during prolonged Na/K pump blockade. It is also shown that Na/Ca exchange can contaminate measurements of Na/K pump currents under a variety of experimental conditions. The way in which these and other functions are affected by the dissociation constants and total capacity of the intracellular calcium buffers are also explored in detail.

Address reprint requests to Dr. Richard P. Kline, Department of Pharmacology, College of Physicians and Surgeons, Columbia University, 630 West 168th Street, New York, NY 10032.

J. GEN. PHYSIOL. © The Rockefeller University Press · 0022-1295/90/03/0499/24 $2.00
Volume 95 March 1990 499–522

INTRODUCTION

Early attempts to describe the transmembrane movement of ions across the cardiac sarcolemma examined the rapid ionic currents that occur during voltage-clamp steps (McAllister et al., 1975) or the slow shifts in cellular ion content measured with radiolabels or other analytic techniques that monitor total cell ion content with time (Niedergerke, 1963; Langer, 1964). Subsequently the contribution of electrogenic transport to the transmembrane potential was pursued (Gadsby and Cranefield, 1979; Falk and Cohen, 1984); at the same time the influence of rapid voltage-activated current fluxes on the transmembrane ionic balance was considered (Atwell et al., 1979; Kootsey et al., 1980; Levis et al., 1983). Thus, intracellular sodium and calcium loading (Eisner et al., 1981*a*; Cohen et al., 1982; Sheu and Fozzard, 1982; Ellis, 1985; Boyett et al., 1987) and extracellular potassium accumulation and depletion (Cohen and Kline, 1982; Kline and Kupersmith, 1982) were seen as routine consequences of repeated activation of transient transmembrane currents. Subsequent attempts (Deitmer and Ellis, 1980; Ellis and MacLeod, 1985; Piwnica-Worms et al., 1985) to include the role of both single ion and coupled transport systems (electrogenic and nonelectrogenic) analyzed in some detail the interaction of these multiple active and passive transport systems, showing, for example, that ions could be effectively coupled by sharing common cotransport partners even when not actually transported by the same molecular entity (Jacob et al., 1984).

Furthermore, recent examination of two of the ions (hydrogen and calcium), frequently studied for their role in carrying charge across the membrane, have suggested a further complication. These ions are not only transported across the membrane, but buffered intracellularly as well (DiFrancesco and Noble, 1985). This buffering by both specific subcellular organelles and diffuse cytoplasmic constituents has a profound effect in converting a net transmembrane movement of the ion into an actual change in ionic activity. In many cases the change in ionic activity, which is critical for regulating transmembrane fluxes at the exchangers (Mullins, 1981), is many orders of magnitude smaller than predicted by net transmembrane flux alone (Brinley et al., 1978; Baker and Umbach, 1987).

A specific example that we consider here is the influence of intracellular Ca^{++} buffering on the activity of the Na/Ca exchanger (Bridge, 1986; Chapman, 1986; Hodgkin et al., 1987). The activity level of intracellular Na^{+} in the cardiac cell is four to five orders of magnitude higher than that of calcium. (For reviews of these measurements, on $a\mathrm{Na}_i$, see Walker 1986, and on $a\mathrm{Ca}_i$, see Blinks, 1986). Thus, after changes in the transmembrane sodium gradient, the exchanger can be kept at equilibrium by a relatively small change in intracellular calcium activity. However, if the capacity of the intracellular calcium buffering is large, this small change in calcium activity may require millimolar changes in total calcium concentration. However, Ca^{++} buffering is not infinite, and therefore attributing to the Na/Ca exchange with a Ca^{++} buffer system the ability, for example, to compensate for a blocked Na/K pump (Deitmer and Ellis, 1978*a*, *b*; Mullins, 1981; Eisner et al., 1983*b*) may be unwarranted. Here we examine by computer simulation and analytic approximation the interaction in resting heart between sarcolemmal Na/Ca exchange, Na influx, and a Na/K ATPase pump in the presence of just one soluble

intracellular calcium buffer at a constant membrane potential. In some simulations a Ca-ATPase pump is also present.

The model enables us to examine the effect of buffer K_d and total buffering capacity on the behavior of transmembrane calcium movements. We also examine, using both the model and analytical approximations, the effects of other parameters related to Na/Ca exchange, Na/K ATPase and Ca-ATPase pumps and transmembrane passive fluxes. Our results suggest that the Na/Ca exchanger cannot substitute for the Na/K pump completely except for very short time periods, unless the intracellular buffering has an unreasonably high capacity, or unless there is a Ca-ATPase pump. On the other hand, even for normal estimates of intracellular Ca^{++} buffering, the Na/Ca exchanger can alter the time course of changes in $a\mathrm{Na}_i$ induced by changes in maximal Na/K pump rate or changes in passive flux.

GLOSSARY

$a\mathrm{Na}_i$	Intracellular sodium activity
$a\mathrm{Ca}_i$	Intracellular calcium activity
$[\mathrm{Na}]_o$	Extracellular sodium concentration
$[\mathrm{Na}]_i$	Intracellular sodium concentration
$[\mathrm{Na}]_s$	Initial intracellular sodium concentration
$[\mathrm{Ca}]_o$	Extracellular calcium concentration
$[\mathrm{Ca}]_f$	Intracellular free calcium concentration
$[\mathrm{Ca}]_{tot}$	Total intracellular calcium
ICS	Intracellular space volume
B_t	Total calcium buffer capacity
K_{Ca}	K_d of calcium buffer
K_{Na}	K_d of intracellular sodium-binding site of Na/K ATPase pump
K_C	K_d of intracellular calcium-binding site of Ca-ATPase pump
M_p	Maximal velocity of Na/K ATPase pump as change induced in intracellular concentration in millimolar sodium/second
M_x	Velocity of Na/Ca exchanger as change induced in intracellular concentration in millimolar calcium/second per millivolt exchanger displacement from equilibrium
M_C	Maximum velocity of Ca-ATPase pump as change induced in intracellular concentration in millimolar calcium/second
j, j_0	Sodium passive leak rate and leak rate for initial conditions as change induced in intracellular concentration in millimolar/second
H	Apparent sodium leak rate as fraction of j
j_{Ca}	Constant calcium inward current as change induced in intracellular concentration in millimolar calcium/second
V_m	Membrane potential in millivolts
V_x	Equilibrium potential of Na/Ca exchanger
V_{Na}	Sodium equilibrium potential
V_{Ca}	Calcium equilibrium potential
RT/F	The gas constant (R) and Faraday's constant (F) have their usual meanings. T is the temperature in degrees Kelvin.
I_p	Na/K ATPase pump current
$\mathbf{C}$	Vector field of $(\mathrm{d}[\mathrm{Na}]_i/\mathrm{d}t, \mathrm{d}[\mathrm{Ca}]_{tot}/\mathrm{d}t)$

METHODS

The model simulates in resting heart the interaction of a passive sodium leak, a sarcolemmal Na/K ATPase pump, a sarcolemmal Na/Ca exchanger, and a simple saturable intracellular calcium buffer. In some simulations a Ca-ATPase pump was added. Each simulation starts in steady state. The Na/K pump is then eliminated and intracellular sodium rises to some predetermined value, at which point the Na/K pump is reactivated. During the interim period the Na/Ca exchanger extrudes Na^+ coupled to Ca^{++} influx. The Ca^{++} then interacts with a simple buffer.

We used several assumptions in developing this model. They are mentioned here and considered in some detail in the discussion. First, we assume the sodium influx is constant. Some simulations used an ohmic current, with results showing no fundamental differences.

Second, we assume the rate of the Na/Ca exchanger is a linear function of the driving force acting on the exchanger (the difference between the membrane potential, V_m, and the exchanger equilibrium potential V_x; see below and Mullins, 1981). Recent direct measurements (Kimura et al., 1987) and theoretical studies (e.g., Eq. 26, DiFrancesco and Noble, 1985; Eq. pg. 42, Mullins, 1981) indicate a more complex dependence on the exchange driving force, but one which is still reasonably linear for driving forces predicted by this model. Without more detailed knowledge of the exchanger binding properties (Johnson and Kootsey, 1985), these more complex equations do not help define the nature of the deviation from linearity.

Third, we model the Na/K pump rate as a saturating, noncooperative, cubic in $[Na]_i$, (Baumgarten and Desilets, 1987; Cohen et al., 1987*b*). Fourth, we assume the stoichiometries for the two transport systems are fixed at 3:2 (Na:K) for the Na/K pump and 3:1 (Na:Ca) for the Na/Ca exchanger. Finally, we use free ion concentrations in all calculations, rather than activity (Tsien and Rink, 1980). We also assume, for simplicity, that sodium buffering and sequestration is negligible and that total sodium per liter of intracellular space is equivalent to free sodium concentration.

The model is run as follows. The sodium leak rate (j_0) at the assumed membrane potential (V_m), the initial intracellular sodium concentration ($[Na]_s$), and the half saturation value for the Na site of the sodium pump (K_{Na}) are provided. These parameters are employed to calculate the maximum flux rate of the Na/K pump (M_p) required for the initial steady state:

$$M_p = j_0 \left(\frac{[Na]_s + K_{Na}}{[Na]_s} \right)^3 \tag{1}$$

The intracellular free calcium concentration ($[Ca]_f$) is then calculated by assuming that the Na/Ca exchanger is in equilibrium, as follows:

$$[Ca]_f = [Ca]_o \left(\frac{[Na]_i}{[Na]_o} \right)^3 \exp\left(\frac{V_m F}{RT} \right) \tag{2}$$

$[Ca]_f$ is assumed to be stabilized by a buffer with dissociation constant K_{Ca} and total buffering capacity, B_t, from which the total internal calcium ($[Ca]_{tot}$) is calculated:

$$[Ca]_{tot} = [Ca]_f \frac{[Ca]_f + K_{Ca} + B_t}{[Ca]_f + K_{Ca}} \tag{3}$$

The V_{max} of the exchanger (M_x) is provided. The value for the maximum Na/K pump rate is then reduced to zero. $[Na]_i$ starts to increase, displacing the equilibrium potential (V_x) of Na/Ca exchanger from its original value at the clamped membrane potential (V_m). The Na/Ca exchanger responds by pumping Na^+ out and Ca^{++} in at a rate proportional to the displacement from its equilibrium.

The computation then proceeds by a fourth order Runge-Kutta integration of:

$$\frac{d[Na]_i}{dt} = j - 3M_x(V_m - V_x) \tag{4}$$

and

$$\frac{d[Ca]_{tot}}{dt} = M_x(V_m - V_x) \tag{5}$$

under the condition of Eq. 3. From Eq. 2:

$$V_x = \frac{RT}{F} \ln\left[\frac{[Ca]_f}{[Ca]_o}\left(\frac{[Na]_o}{[Na]_i}\right)^3\right] = 3V_{Na} - 2V_{Ca} \tag{6}$$

The computation continues until the internal sodium concentration reaches a preset critical value, at which point the sodium pump term

$$-M_p\left(\frac{[Na]_i}{K_{Na} + [Na]_i}\right)^3 \tag{7}$$

is returned to the right-hand side of Eq. 4 for calculating the rate of change of internal sodium. The integration proceeds until 500 points have been calculated at a preset sampling interval. The decay of $[Na]_i$ was fit to one or two exponentials for comparison to values of these parameters in the literature. Fits were performed using BMDP Statistical Software (Program "3R", Nonlinear Regression; University of California Press, 1985). $[Ca(t)]_f$ is calculated by solving Eq. 3. We also examine the driving force on the Na/Ca exchanger.

In some simulations, a Ca-ATPase pump was present. It was modeled as a saturating function of $[Ca]_f$ with a dissociation constant (K_C) of 0.3 μM (Caroni and Carafoli, 1981) for all simulations. The maximum velocity (M_c) varied from 2 to 12.5 μM/s, the latter being one half the influx value assumed for Na^+ at rest. We added a constant inward calcium leak (j_{Ca}) to Eq. 5 such that j_{Ca} balanced the Ca-ATPase flux for the initial value of $[Ca]_f$. For such situations Eq. 5 becomes:

$$\frac{d[Ca]_{tot}}{dt} = M_x(V_m - V_x) + j_{Ca} - M_C\left(\frac{[Ca]_f}{[Ca]_f + K_C}\right) \tag{8}$$

All fluxes are expressed in units of concentration per unit time. They can be readily converted to units of quantities per membrane area per unit time by knowing the surface to volume ratio of the cells and the liters of water per liter of cell volume. If we tentatively assume that the addition of one mole per liter of cell volume gives a 1 molar change in concentration; then as a rule of thumb, for surface-to-volume ratios between 1.0 and 0.1 μm^{-1} each 1.0 pmol/cm^2/s of transmembrane flux gives a rate of intracellular concentration change of 1.0–10.0 μM/s. For long cylindrical cells, this range of surface to volume ratios corresponds to radii of 2–20 μm.

The computer model of DiFrancesco and Noble (1985) includes all the major passive ion currents, a Na/K ATPase pump, a Na/Ca exchanger, a small intracellular compartment that accumulates and releases Ca^{++} (designed to simulate the sarcoplasmic reticulum), but no Ca-ATPase pump. Some of the simulations presented here should be reproducible using the software for this model after making appropriate adjustments in their parameter values.

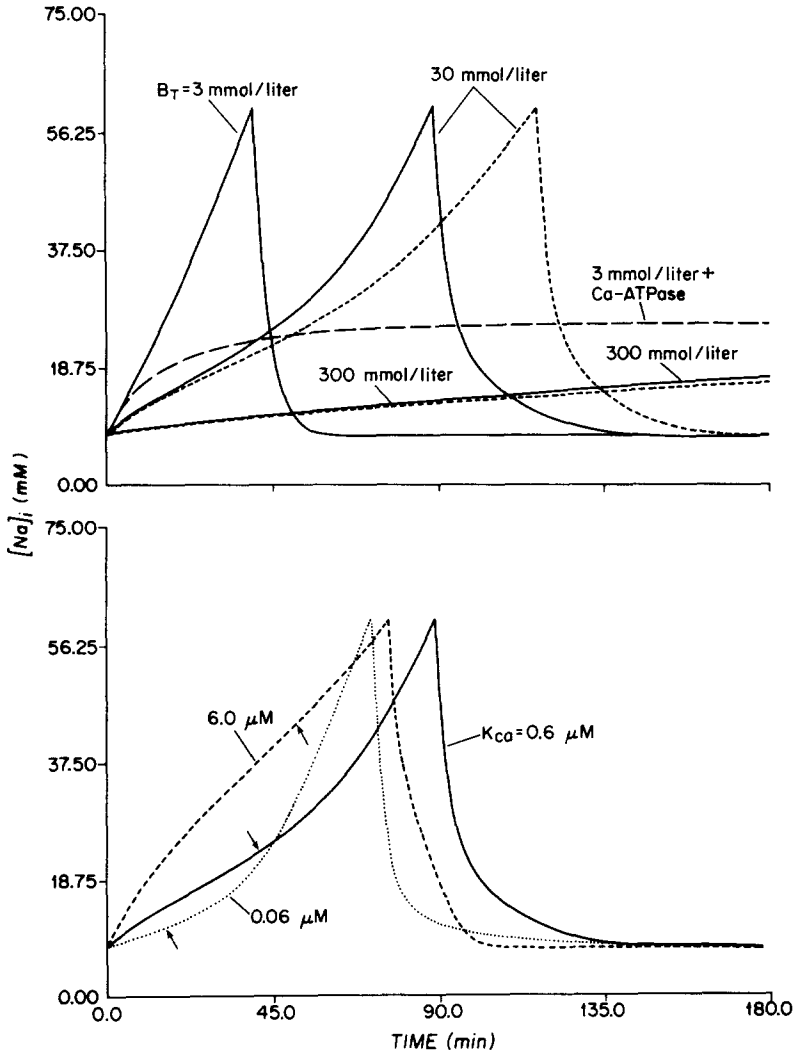

FIGURE 1. The effect on sodium loading of varying total buffer concentration, B_t, and buffer binding constant, K_{Ca}, are shown in the upper and lower panels, respectively. The upper panel demonstrates the effect of increasing total buffer (B_t) from 3 to 30 to 300 mmol/liter (left to right, *solid lines*). Note that B_t values larger than any reasonable estimates cannot prevent the $[Na]_i$ rise. We also assumed an ohmic leak, but still were unable to prevent the $[Na]_i$ rise for the case of the two largest total buffer concentrations (30 and 300 mmol/liter, *short-dashed lines*). Yet the addition of the Ca-ATPase pump (*broken line*), even for the smallest B_t value (3 mmol/liter) and constant Na^+ influx, allows for complete cessation of the Na^+ loading. The Ca-ATPase pump has a maximum velocity of 12.5 μM/s and a binding constant of 0.3 μM. This illustrates the capability of a Ca-ATPase pump with a maximum velocity greater than one-third the Na^+ leak to halt sodium influx in concert with a Na/Ca exchanger. Other model parameters are: $V_m = -50$ mV; $[Na]_s = 8$ mM; $K_{Na} = 12$ mM; $K_{Ca} = 0.6$ μM; $[Na]_0 = 160$ mM; $[Ca]_0 = 2$ mM; and $M_x = 1.8$ μM/mV per s. The lower panel simulates Na^+ loading with K_{Ca}'s of 0.6 (*solid line*), 6.0 (*dashed line*) and 0.06 μM (*dotted line*) for a buffer with

RESULTS

Buffer Capacity and the Rate of Increase of $[Na]_i$

When the Na/K pump is blocked, $[Na]_i$ increases. We used the computer model to examine the extent to which the Na/Ca exchanger maintains sodium homeostasis during Na/K pump suppression, albeit at an elevated level (Deitmer and Ellis, 1978*a*, *b*; Mullins, 1981). We found that unrealistically large values of B_t (the total buffer capacity) are required to sustain a nearly flat plateau for 30 min. For values of total buffer normally associated with reversible cellular buffering, the exchanger can reduce the rate of net Na^+ influx, but only for brief periods until the calcium buffer is saturated. When the buffer is saturated, net Na^+ influx proceeds at rates nearly equal to the passive flux.

Fig. 1 (*top*) shows trajectories for $[Na]_i$ vs. time for total buffer capacities of 3, 30, and 300 mmol/liter intracellular space. The lowest buffer value represents rapidly reversible buffering seen during physiologically normal circumstances (1–5 mmol/liter ICS; Langer, 1964, 1974; Bridge, 1986; Fintel and Langer, 1986). The next largest value represents an average estimate for intact cells during nonphysiologic experimental interventions, such as high doses of glycosides (Bridge and Bassingthwaighte, 1983; Murphy et al., 1983), reduced $[Na]_o$ (Langer, 1964; Carafoli, 1973; Chapman et al., 1983), or application of permeabilizing agents (Fry et al., 1984*a*, 1987). This intermediate range of values (6–40 mmol/liter ICS) is primarily mitochondrial buffering. The largest value represents extrapolation from isolated mitochondrial experiments under conditions designed to maximize mitochondrial uptake (Greenwalt et al., 1964; Carafoli, 1973; based on estimate from Carafoli, 1985, that the ratio of cardiac tissue wet weight to weight of mitochondrial protein is 10:1). The largest value is most likely a substantial overestimate.

To eliminate the possibility that this conclusion about required buffer capacity is due to underestimating Na/Ca exchanger maximum velocity (M_x), we used a value for M_x of 1.8 μM/mV displacement from equilibrium per second. This is a saturating value in that higher values generated little further change in outcome (as will be shown in Fig. 2).

To account for a possible reduction in Na^+ passive influx as $[Na]_i$ rises we repeated the simulations for the two largest buffer capacities for the case of an ohmic Na^+ influx (Fig. 1, *top, short dashed traces*). These two alternatives should cover the range of reasonable experimental possibilities, since a third alternative, assuming a constant P_{Na} and independence (Eisner et al., 1981*a*) leads to smaller effects of

---

B_t = 8 mmol/liter. The starting $[Ca]_f$ is 0.03 μM, calculated at the exchanger equilibrium for the parameter values used. Since the exchanger most effectively suppresses the leak for $[Ca]_f \simeq K_{Ca}/2$ (see Appendix), the suppression of the leak is most effective at the start of the loading for the smallest K_{Ca} (0.06 μM). The buffer with intermediate K_{Ca} (0.6 μM) allows aNa_i to rise more rapidly initially; then the rate of rise is reduced, followed by eventual failure of suppression as the buffer becomes full. With a K_{Ca} of 6.0 μM, the buffer-exchanger action has minimal effect on Na^+ influx initially, and only reaches maximum influx suppression just before reactivation of the pump. Maximum suppression of Na^+ influx is indicated by arrows on all curves.

changes in $[Na]_i$ on Na^+ influx than the ohmic alternative (Cohen et al., 1987*a*). Thus the constant field approximation should give results between those of a constant leak and an ohmic leak. This modification still did not allow for complete suppression of the $[Na]_i$ rise.

In all cases, even for assumed total cell calcium buffers (B_t) of several hundred mmol/liter, a $[Na]_i$-dependent reduction in Na^+ passive influx, and very large exchanger capacities (M_x), the continued rise of $[Na]_i$ could not be suppressed. The reason is that exchanger extrusion of Na^+ necessarily implies exchanger-mediated Ca^{++} influx. This would cause V_{Ca} to decrease unless $[Ca]_f$ were perfectly buffered. The driving force on the Na/Ca exchanger ($V_m - V_x = V_m - 3V_{Na} + 2V_{Ca}$) would then also decrease unless $[Na]_i$ continued to rise. However, for any physiologic values of intracellular calcium buffering there is sufficient slow increase in $[Ca]_f$ to prevent both a constant exchanger driving force and stabilization of $[Na]_i$.

If the Na/K pump were blocked, but Ca-ATPase–mediated transport were still functioning, then a relatively constant $[Na]_i$ could readily be sustained providing the Ca-ATPase flux were sufficiently large to counter the Ca^{++} influx due to the Na/Ca exchanger. To hold $[Na]_i$ at a plateau indefinitely, the Ca-ATPase efflux must equal one-third of the Na^+ influx. This would allow for extrusion of all the Ca^{++} brought in by Na/Ca exchange.

The effect of a Ca-ATPase pump with V_{max} of 12.5 μM/s (i.e., $> j_0/3 = 8.334$ μM/s) is also illustrated Fig. 1 (*top, broken trace*), for the smallest buffer capacity (3 mmol/liter). For all V_{max} values of Ca-ATPase $> j_0/3$, stable plateaus in $[Na]_i$ occur. Even with only 30 μmol/liter total calcium buffers (not shown), the rate of sodium rise can be slowed and eventually stopped. In the absence of a Ca-ATPase pump, and in the presence of a Na/Ca exchanger, 30 μmol/liter Ca^{++} buffer has essentially no effect on the rate of increase of $[Na]_i$. Likewise, no matter how large the Ca-ATPase flux, in the absence of Na/Ca exchange the Ca-ATPase has no effect on the rate of $[Na]_i$ rise after pump blockade.

Effects of Varying Buffer K_d

For a given set of initial conditions, the starting value of sodium defines the starting value of $[Ca]_f$ and $[Ca]_{tot}$. In the simulation, the rate of change of $[Na]_i$ with time depends on the value of $[Ca]_f$ relative to the K_d of the buffer (K_{Ca}). This relation determines the percent occupancy of the buffer, and the rate of change of $[Ca]_f$ and V_{Ca} as a function of the turnover rate of the Na/Ca exchanger. We examined, using the model and analytical approaches, whether there was a consistent relationship between $[Ca]_f$ and K_{Ca} at the point where the greatest suppression of sodium flux by the Na/Ca exchanger occurred. We found that the exchanger has its maximum influence when $[Ca]_f$ is approximately equal to 0.5 K_{Ca} (i.e., the buffer is approximately one-third occupied; see Appendix). We therefore expect that during Na/K pump blockade and constant passive influx (j_0), the rate of rise of $[Na]_i$ will transiently attain a minimum value at a predictable point, as illustrated in the bottom panel of Fig. 1.

If the initial $[Ca]_f$ is much smaller than K_{Ca}, $[Na]_i$ will rise rapidly, then slow, then rise rapidly again (Fig. 1, *dashed and solid traces*). If the initial $[Ca]_f$ is slightly less than or equal to 0.5 K_{Ca}, the greatest suppression of $[Na]_i$ increase will occur at the start

of the $[Na]_i$ rise immediately after the Na/K pump is blocked (*dotted trace*). The buffer will fill sooner than for higher K_{Ca}; once the buffer is filled, $[Na]_i$ will rise rapidly. If the starting $[Ca]_f$ is much larger than K_{Ca}, the opportunity to suppress the $[Na]_i$ rise is lost and $[Na]_i$ rises more rapidly as the buffer continues to fill.

Effects of Altering Exchanger Capacity

Since the absolute magnitudes of the transmembrane fluxes of the exchanger are not yet well described (Philipson and Ward, 1986), it is worth considering how variations in the maximum fluxes of the exchanger might influence these results. Fig. 2 shows the effects of varying M_x on the $[Na]_i$ time plots. Increasing M_x to values >1.8 μM/s per mV displacement from exchanger equilibrium does not appreciably alter the $[Na]_i$ and $[Ca]_f$ trajectories. Likewise the time plots approach limiting trajectories for values <0.0018 μM/s per mV displacement from exchanger equilibrium. Within the range between these values, both the rate of rise of $[Na]_i$ upon Na/K pump blockade, and the time constants of the $[Na]_i$ decay after pump reactivation vary considerably (see Appendix).

Modeling output for $[Na]_i$, $[Ca]_i$, and exchanger driving force ($V_m - V_x$) is shown in Fig. 2. A steady state in $[Na]_i$ is established by balancing Na^+ passive influx with Na/K pump extrusion, and for $[Ca]_f$ by requiring the exchanger to be in equilibrium. The Na/K pump is blocked and $[Na]_i$ (Fig. 2, *top*) rises, inducing a rise in $[Ca]_f$ (*middle*).

Initially, the exchanger equilibrium implies that the driving force is zero. As $[Na]_i$ accumulates, the driving force on the exchanger becomes progressively more positive (Fig. 2, *bottom*) until a maximum value is reached for exchanger-mediated efflux of Na^+ and influx of Ca^{++}. Subsequent to this maximum, the driving force slowly becomes smaller. When the Na/K pump is reactivated, the $[Na]_i$ falls and the driving force becomes large and negative, indicating that Na/Ca exchanger is extruding Ca^{++}, causing Na^+ influx. This slows the apparent rate of $[Na]_i$ decay.

The maximum reduction of the rate of $[Na]_i$ rise saturates at ~50% of the Na^+ leak rate for the largest exchanger flux capacities and parameter values used in Fig. 2 (see Appendix); these M_x values are associated with only millivolt displacements from equilibrium. For the low end of exchanger flux capacity, reduction of the rate of rise of $[Na]_i$ of only several percent are associated with displacements from equilibrium of over 100 mV. Physiologically relevant flux capacities are estimated at 1.0 μM/s per mV based on a recent study (Kimura et al., 1987; see Discussion).

One effect of Na/Ca exchange on the decay of Na after pump reactivation is to slow the rapid phase normally associated with the Na/K pump. This phase has a time constant of between 50 and 300 s when measured experimentally (Deitmer and Ellis, 1978*b*; Gadsby and Cranefield, 1979; Eisner et al., 1981*a*, *b*; Cohen et al., 1982; January and Fozzard, 1984; Ellis, 1985; Boyett et al., 1987). The model reproduces these time constants and further demonstrates that the addition of a Na/Ca exchanger can slow this initial phase and also generate a slow second component of sodium decay. This second component of $[Na]_i$ decay, when present, has a time constant up to an order of magnitude larger than the rapid phase.

The $[Na]_i$ decay time constant for simulations in Fig. 2 with no exchanger or M_x values below 0.06 μM/s per mV flux capacity was 177 s. This value then increased

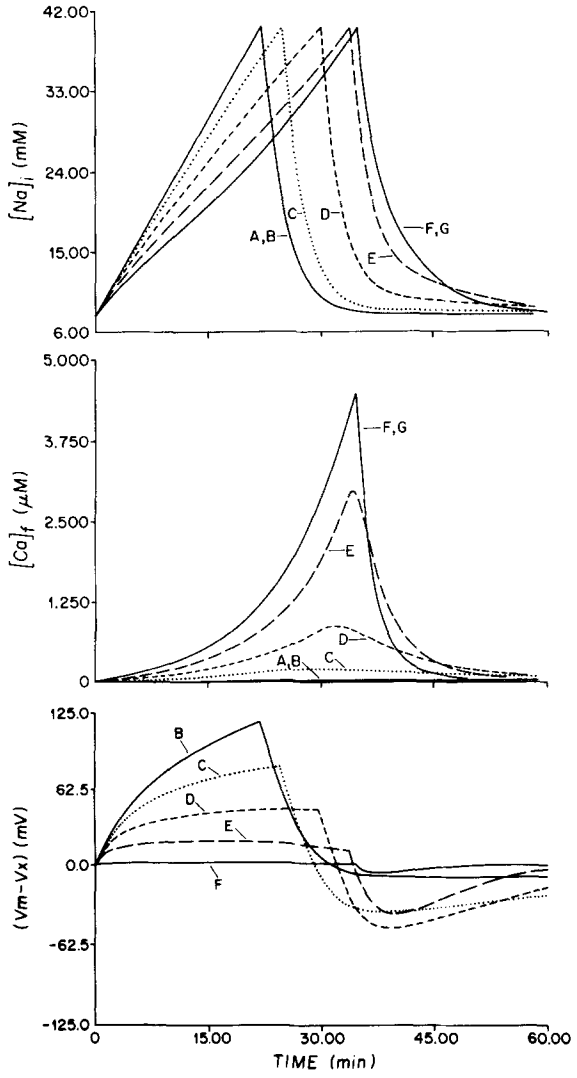

FIGURE 2. Model output is shown simulating Na-ATPase pump blockade followed by pump reactivation. Traces are the time courses of intracellular sodium, $[Na]_i$ (*top*), intracellular free calcium, $[Ca]_f$ (*middle*), and exchanger driving force, $V_m - V_x$ (*bottom*). In traces *A* through *G* the values of the Na/Ca exchanger maximum velocity, M_x, are 0.00018, 0.0018, 0.018, 0.06, 0.18, 1.8, and 6.0 μM Ca^{++}/s per mV displacement from equilibrium, respectively. The rate of sodium loading is successively slowed as M_x increases within this range, but shows no further changes for values outside the range. Single exponentials fit to the sodium decays yield time constants of 177, 177, 177, 199, 280, 308, and 304 s in the same order. Double exponentials could only be fit at the five highest values of M_x, giving values of fast time constant, slow time constant, and ratio of the amplitudes of the slow to the fast components as follows (in the same order): 170 s, 5,000 s, 0.012; 151 s, 1,279 s, 0.10; 125 s, 625 s, 0.486; 73 s, 345 s, 4.5; and 65 s, 326 s, 7.0. Calcium loading increases while the exchanger driving force decreases with higher M_x values. B_t = 8 mM and K_{Ca} = 0.6 μM. All other model parameters used were the same as in Fig. 1. The degree of divergence of the falling vs. rising phases of the trajectory (see text) can be assessed by examining the ratio of their $[Ca]_f$ values for $[Na]_i$ = 20 mM where the effect appears greatest. This ratio for traces *C*, *D*, and *E* is 3.4, 6.7, and 7.2, respectively; whereas it is between 1.0 and 1.4 for all other traces.

up to 308 s for increasing flux capacities. For flux capacities from 0.018 to 0.18 μM/s per mV there was also a second slower component with time constants between 600 and 5,000 s. For the highest exchanger flux capacities, most of the decay was fit by a time constant of 300–350 s with a much smaller (<20%) rapid component of time constant <75 s (see Appendix).

The slowing of the time course of $[Na]_i$ decay does not require large accumulations of Na^+ and Ca^{++}. For example, changing the amount of accumulated Na^+ from 32 (Fig. 2) to 3.2 mmol/liter (not shown) for the simulation with $M_x = 1.8$ μM/s per mV changed the time constant from 307 to 288 s. This still represents a 62% increase over the value with no exchanger present. Even when the total buffer capacity was reduced to 3 mmol/liter ($M_x = 1.0$ μM/s per mV; $K_{Ca} = 1.0$ μM; $V_m = -50$ mV), a 14 and 26% increase in the single exponential time constant was seen for Na^+ accumulations of 3.2 and 32 mmol/liter, respectively.

The effect of the Ca-ATPase pump on the $[Na]_i$ rise was described above (Fig. 1). It is worth mentioning at this point, that over the range of M_x values shown in Fig. 2 the Ca-ATPase pump acts to reverse the lengthening of time constants and development of slow components of $[Na]_i$ decay caused by increasing the Na/Ca exchanger activity.

We have also taken the data generated in Fig. 2 and made time-independent plots of $[Ca]_f$ vs. $[Na]_i$ (not shown). For the largest values of M_x the exchanger is nearly at equilibrium and the plots during the rising and falling values of $[Na]_i$ and $[Ca]_f$ nearly superimpose, as they do (although on a different trajectory) for the smallest values of M_x where the exchanger has no influence. For the intermediate values of M_x, the rising and falling legs do not superimpose (Fig. 2, traces *C*, *D*, and *E*; see caption). However, the $[Ca]_f$ lags the $[Na]_i$, suggesting that tension and the transient inward current (which depend on $[Ca]_f$) should be higher for a given $[Na]_i$ during the falling rather than the rising phases of the $[Na]_i$ changes. This result goes contrary to that required to explain the well known hysteresis of plots of $[Na]_i$ vs. tension (Eisner et al., 1981*a*) and $[Na]_i$ vs. transient inward current (Eisner et al., 1983*a*), and implies that Ca^{++} buffering cannot account for this effect. If one assumed a similar hysteresis in pH_i vs. $[Na]_i$ (perhaps mediated by Na/H exchange), this could account for the results since reducing pH_i suppresses tension (Vaughn-Jones et al., 1987). However, the complex dependence of tension on parameters outside the scope of this model allows for many alternative explanations.

DISCUSSION

General Conclusions

We have studied the relationship between $[Na]_i$, $[Ca]_i$, and $[Ca]_{tot}$ in a computer simulation. During periods of increased net Na^+ influx due to Na/K pump suppression, Na/Ca exchange (a coupled transporter with energy derived primarily from ionic gradients) can, for a period of time, partially substitute for the Na/K pump by extruding Na^+ at the cost of cellular Ca^{++} gain. However, the Na/Ca exchanger cannot reduce net Na^+ influx totally or continue to counter passive Na^+ influx for prolonged periods of time. It can temporarily make a significant contribution providing there is a large intracellular buffer capacity or an additional transporter that extrudes Ca^{++} without coupling to Na^+ influx (e.g., the Ca-ATPase driven sarcolemmal Ca^{++} pump). The exchanger is most effective in countering Na^+ net flux when the buffer is approximately one-third filled (see Appendix).

When the Na/K pump is reactivated, there is a rapid $[Na]_i$ decay similar to that reported in the experimental literature (Cohen et al., 1982; Ellis, 1985). The time constant of this phase is dependent on the kinetics of the Na/K pump, but can be

significantly altered by the Na/Ca exchanger. The variation in this time constant during interventions that wouldn't ordinarily be expected to affect the Na/K pump (Ellis, 1985; Boyett et al., 1987) may be due to modulation of $[Na]_i$ decay by the exchanger. Since both the Na/K pump and the Na/Ca exchanger transport three Na ions in the direction of one positive charge, it is not unreasonable to expect, as has been observed, a parallel decay in the rate of $[Na]_i$ extrusion- and transport-related currents (Eisner et al., 1981*a*) even with both transporters operating.

The initial fall in $[Na]_i$ can reverse the driving force on the Na/Ca exchanger so that it functions in the Ca^{++}-efflux, Na^+-influx mode. As the $[Na]_i$ falls due to the activated Na/K pump, the Na/K pump rate falls. At the same time, the driving force on the Na/Ca exchanger increases. To the extent that the Na^+ fluxes generated by the two transport systems balance, the $[Na]_i$ decay is slowed. Before the reversal of the exchanger driving force, there is a brief period during which the exchanger and the Na/K pump are both extruding Na^+. This showed up as a small component of Na^+ decay with a very rapid time course (see caption, Fig. 2).

Simplifying Assumptions about the Buffer

The model includes several simplifying assumptions about the buffer. We assumed a saturable buffer with a single binding site. There are many intracellular sites of calcium buffering, for example: parvalbumin, calmodulin, myosin, troponin, calsequestrin, sarcoplasmic reticulum, inner surface of sarcolemma membrane, and mitochondria (Robertson et al., 1981; Fabiato, 1983). They vary widely in terms of their active or passive nature, affinity, time dependence, and total capacity. We decided to characterize the simplest case first. Ca^{++} buffers can be cooperative. As the degree of cooperativity increases, it should be easier to create a plateau, although the plateau's duration is still limited.

In our model we ignored the rapid kinetics of buffering that determines the time dependence of calcium transients during a single twitch (Robertson et al., 1981; Fischmeister and Horackova, 1983). We also ignored the time dependence of mitochondrial transport, as well as other complexities of mitochondrial transport such as the dependence on intracellular sodium, pH_i, and magnesium, and availability of oxygen and substrates (Fry et al., 1984*b*).

Normally, total cell calcium is one to several mmol/kg wet tissue weight (Langer, 1964, 1974; Bridge, 1986; Fintel and Langer, 1986). However, total cell calcium may be as large as 6–40 mmol/liter ICS during experimental interventions designed to load Ca^{++} (Bridge and Bassingthwaighte, 1983; Murphy et al., 1983; Langer, 1964; Carafoli, 1973; Chapman et al., 1983; Fry et al., 1984*a*, 1987). Most of this calcium is held in mitochondria which have a substantial reversible buffering capacity (Carafoli, 1973). There is a large irreversible component of mitochondrial Ca^{++} buffering inherent in the ability to precipitate quantities of calcium phosphate. Aside from the mitochondria, the remaining intracellular Ca^{++} buffering is on the order of one to several mmol/liter.

Quantitative Assumptions about Transport Fluxes

Comparative transport rates of the Na/K pump, the Na/Ca exchanger, and the Ca-ATPase pump are required to establish physiological ranges of these parameters in the model. We assumed resting Na/K pump fluxes sufficient to balance passive

influx capable of generating $[Na]_i$ changes of 1.5 mM/min (25 μM/s). This is probably a high estimate since the literature values range from 0.5 to 1.5 mM/min (8.33–25 μM/s; converted to concentration from activity by assuming 0.74 activity coefficient). If we assume a surface to volume ratio of 0.4 μm^{-1} these values are consistent with membrane flux estimates of 2–6 pmol/cm^2 per s (Eisner et al., 1981*a*, *b*; Chapman et al., 1983; Glitch and Pusch, 1984; Cohen et al., 1987*a*, *b*). In order for the Na/Ca exchanger to substitute for the Na/K pump as a Na^+ extruder, we require that it generate comparable Na^+ efflux, or Ca^{++} influx of one-third of this magnitude (2.77–8.33 μmol/liter per s; exchanger stoichiometry of 3:1 assumed). Comparable Ca^{++} efflux would be required of the Ca-ATPase pump to keep the buffer from filling.

Estimates of Na/Ca exchanger flux range from a small fraction, to values in excess of the average Na/K pump flux estimates; however, Na/Ca exchange flux estimates are often obtained under nonphysiologic conditions designed to maximize Na/Ca exchanger current (Philipson and Ward, 1986). For example, Philipson and Ward (1986) show from studies on the Ca^{++}-efflux/Na^{++}-influx exchanger mode in vesicles that maximum Na/Ca exchange fluxes (25 nmol/mg vesicle protein per s) are more than those obtained (0.7 nmol/mg vesicle protein per s) when physiologic values of intracellular magnesium, sodium, and pH are used. The authors convert their values to induced intracellular concentration changes of 0.8–1.5 μmol Ca^{++}/kg wet tissue weight per s. If we assume ICS water is 60% of wet tissue weight, this reduces to values of 1.33–2.50 μmol Ca^{++}/liter ICS H_2O per s.

The maximum Na/Ca exchanger–induced Ca^{++} influx of 25 nmol/mg vesicle protein per s (or 40–76 μmol Ca^{++}/liter ICS per s) is as much as an order of magnitude greater than that required to counter the quiescent Na^+ influx we assumed. We are looking at the Ca^{++} influx/Na efflux mode in our model under relatively physiologic conditions, and we may expect values intermediate between the two estimates for the actual Na/Ca fluxes.

After maximal loading of intracellular Na^+ with glycosides and divalent free perfusate (Chapman et al., 1986), the reintroduction of Ca^{++} to the perfusate at high concentration generates very large Na/Ca exchanger fluxes. Under these conditions, Bridge and Bassingthwaite (1983) reported that cells load 6.9 mmol Ca^{++} and extrude 20.6 mmol of Na^+ per kilogram cell water in 10 min. These flux values (~11.5 μmol Ca^{++}/liter ICS per s) could totally suppress even the highest estimated inward passive Na^+ flux assumed in our model, if $[Ca]_f$ were not allowed to change (i.e., were it perfectly buffered). Chapman et al. (1983) likewise found Na/Ca exchange fluxes that exceeded by severalfold the passive Na^+ leak rates.

Philipson and Ward (1986) also measured Ca-ATPase mediated Ca^{++} efflux capacity (1 nmol/mg vesicle protein per s) to be comparable to the estimated "physiologic" Na/Ca exchange flux values above. The calculated Ca-ATPase–induced Ca^{++} efflux is 1.63–3.33 μmol Ca^{++}/liter ICS per s. Using the above assumptions, we can convert data from other studies (Carafoli, 1985; Sanchez-Armass and Blaustein, 1987, in synaptasomes) to the appropriate units and obtain Ca-ATPase fluxes of 1–4 μmol/liter ICS per s, and higher (Barry et al., 1986). The calculated Ca-ATPase–induced Ca^{++} efflux of 1–4 μmol Ca^{++}/liter ICS per s would allow continued Na/Ca suppression of 12–144% of quiescent Na^+ influx without cellular accumulation of calcium.

Thus, although various authors have pointed out that maximum Na/Ca exchanger fluxes are likely to be from 5–60 times larger than those for Ca-ATPase pumps (Carafoli, 1985; Barry et al., 1986; Sheu and Blaustein, 1986), it may still be that Ca-ATPase is sufficient to pump out the Ca^{++} brought in by Na/Ca exchange during reduced Na/K pump activity. This is especially true if passive Na^+ influx decreases as $[Na]_i$ increases. Thus if we assume a Hodgkin-Goldman-Katz Na^+ channel, a membrane depolarization from -80 to -35 mV and a Na^+ activity increase to 30 mM, the Na^+ influx (j) would fall by one half, making it more likely that the Ca-ATPase could effectively compensate for Na/Ca exchange–mediated Ca^{++} influx and explaining why V_m depolarization would be protective of cellular ion gradients.

Exchanger Displacement from Equilibrium

Experimental data from which we can estimate exchanger M_x is available in Kimura et al. (1987), which yields a value of 1.18 μM/s per mV displacement from equilibrium. The estimate is based on their measurements of exchanger current, combined with their cell size (20 pl), V_m, and ion concentrations, and can also be derived by differentiating with respect to voltage their Eq. 3 for V_m equal to -50 mV. This M_x value implies that a 7-mV deviation from exchanger equilibrium could provide an adequate flux to balance the Na^+ passive influx assumed in this model, although in larger cells (e.g., cardiac Purkinje myocytes) and with the theoretical exchanger model of DiFrancesco and Noble (1985; Eq. 26) this balance would require a driving force of as much as 55 mV. Sustained deviations from equilibrium of half this latter amount could explain a decrease (from 3.0 to 2.6) in the estimates of the exchanger stoichiometric ratio based on steady-state ion activity measurements (see Axelson and Bridge, 1985; Sheu and Fozzard, 1985; Sheu and Blaustein, 1986; for this calculation we used Eq. 6 and assumed a ratio of $[Na]_o$ to $[Na]_i$ of 15).

We assumed that the Na/Ca exchanger turnover rate is a linear function of the driving force on the exchanger. Models for the exchanger have been developed with far greater complexity and have a nonlinear dependence on driving force (Kimura et al., 1987, Eq. 3; DiFrancesco and Noble, 1985, Eq. 22). However, Kimura et al.'s experimental description of the driving force dependence of Na/Ca exchanger due to variations in membrane potential is nearly linear (deviations <20%) for driving forces up to 25 mV. Our total displacement from equilibrium is <25 mV for values of $M_x > 0.18$ (which is consistent with both Kimura et al., 1987, and DiFrancesco and Noble, 1985). Stronger nonlinearity may be encountered when the driving force is altered by changing the ion activities and hence the equilibrium potential of the exchanger, rather than by changing the membrane potential. Nevertheless, the nature and amount of such deviations from linearity are not predictable based on available experimental evidence, but are unlikely to be so large as to alter the qualitative conclusions of our model (see for example Fig. 4.3 of Mullins, 1981).

Magnitude of Electrogenic Na/K Pump Currents

Resting pump current, I_p (dihydro-ouabain [DHO]), can be measured by applying a concentration of cardiac glycoside (e.g., DHO) sufficient to block the pump, and measuring the inward movement of membrane current under voltage clamp. A second measure of resting pump current (I_p[0K]) can be obtained by exposing a prep-

aration to K^+-free Tyrode for a time, T, and then returning it to normal Tyrode. The integral (Q) of the additional pump current is then related to the resting pump current (Cohen et al., 1987*a*) by:

$$I_p(0K) = Q/T. \tag{9}$$

I_p(DHO) is an almost instantaneous measure and if Na/Ca exchange is initially at equilibrium, the resting pump current can be measured before the exchanger is moved away from this state. However, I_p(0K) is not instantaneous and relies on the assumption that the Na accumulation intracellularly during pump blockade by K^+-free Tyrode increases I_p above resting levels and mimics that which would occur were all other transports to remain unchanged. However, simultaneous with the increase in $a\mathrm{Na}_i$ is an increase in Na/Ca exchanger activity, reducing the additional increase in $a\mathrm{Na}_i$ by suppressing the Na^+ influx. Thus, the pumped Na^+ efflux (equal to $3Q$) will tend to underestimate the resting Na^+ influx that would occur with the Na/Ca exchanger at equilibrium. The net result is that I_p(DHO) should exceed I_p(0K). In isolated Purkinje myocytes the ratio of I_p(DHO)/I_p(0K) is 1.76 (Cohen et al., 1987*a*), which is in agreement with the prediction, and suggests a role for Na/Ca exchange in suppressing Na influx during 0 mM K^+ exposures.

Implications for Cell Survival during Ischemia

The model gives some insights into events during severe ischemia that may determine cell survival. The Na/K pump can derive significant ATP from glycolysis alone (Hasin and Barry, 1984; Ellis and Noireaud, 1987), whereas mitochondrial Ca^{++} sequestration requires O_2. Thus anoxia subsequent to ischemia could reduce the Ca-buffering capacity before a significant reduction in the Na/K pump activity. Murphy et al. (1983) have shown that during glycoside-induced Na/K pump blockade in cell culture without ischemia or anoxia, large amounts of total calcium (10 mM change in $[Ca]_{tot}$) are reversibly taken up by the cell. The cell appears to recover completely several hours after the removal of the Na/K pump blockade. These total calcium levels are comparable to levels seen during severe ischemia where there is significant cell damage. During pharmacologic pump blockade with no ischemia, there is no cell damage noted. This difference in response could be due to a reduction in reversible calcium buffering during ischemia, so that comparable levels of $[Ca]_{tot}$ mask large inequalities in $[Ca]_f$ increase, where $[Ca]_f$ increase is the lethal event (Schanne et al., 1979).

The model shows that without a noncoupled Ca^{++} extruder, Na/Ca exchange, even with considerable Ca^{++} buffering, cannot limit intracellular Na^+ and Ca^{++} for a prolonged period. Once the Ca^{++} buffers are filled, because of either increased net calcium influx or reduction in total buffering, then only a Ca-ATPase pump can prevent Ca^{++} overload. The suppression of Ca-ATPase has been proposed as a critical step in ischemic cell death in cortex (Kass and Lipton, 1986).

APPENDIX

Model Parameter Values and the Influence of Na/Ca Exchange

To avoid an overreliance on model-dependent conclusions and particular choices of parameter values, we describe here two analytic treatments of important components of model

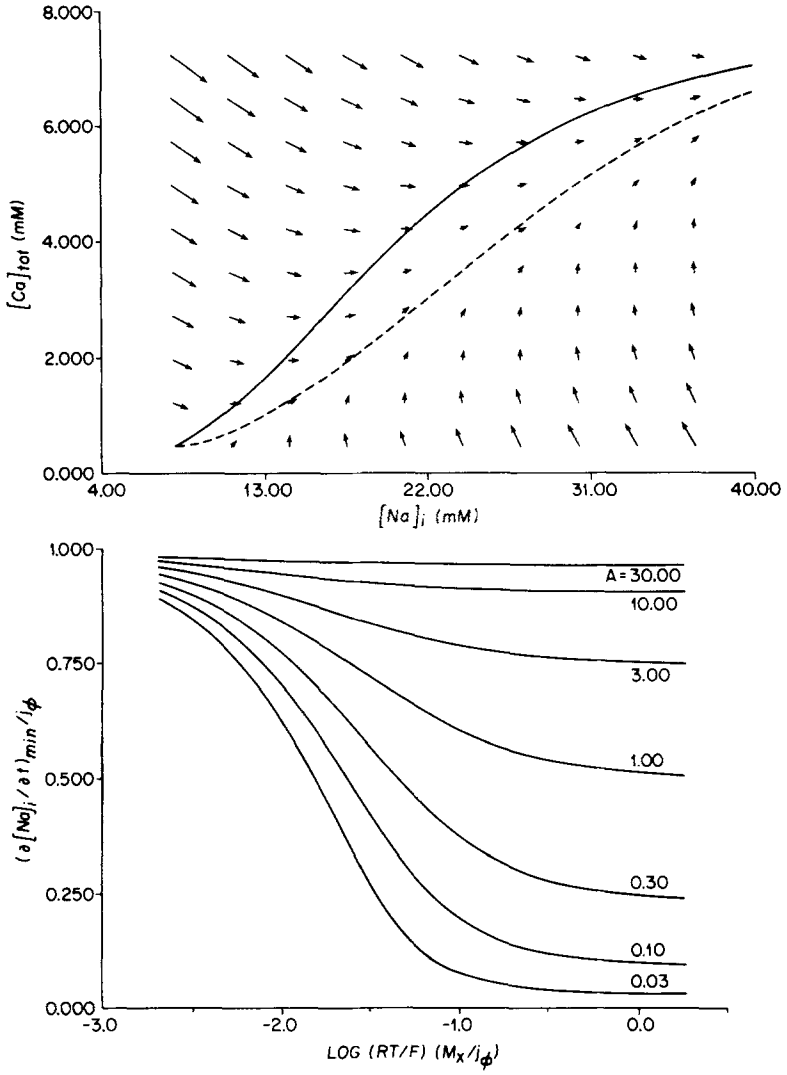

FIGURE 3. (*Top*) The vector field, **C**, whose components are the rates of change of intracellular sodium, $[Na]_i$, and total calcium, $[Ca]_{tot}$, is shown for an array of instantaneous values of these variables. Each arrow represents the direction of the vector field at the origination point of the arrow. Its amplitude is indicated by the size of the arrow. The parameters are identical to trace *E*, Fig. 2. The dashed line corresponds to the phase of sodium loading during Na-ATPase pump blockade. It starts, as do all simulations using this model, with the exchanger at equilibrium. All such equilibrium points are indicated by the solid line. The exchanger driving force is zero along this contour, which is consistent with the fact that all vectors originating from this line are horizontally directed. During a simulation, any trajectory is tangential to the arrows. Although the vector field would differ for alterations in exchanger M_x, trajectories for higher M_x would converge toward the contour (*solid line*), which indicates exchanger equilibrium. Trajectories for lower M_x values would diverge even further from this contour than the trajectory shown. The bottom panel graphs the estimates of the lower bound of the ratio of the apparent Na^+ leak rate ($d[Na]_i/dt$, including exchanger

behavior. The paradigm for exchanger-buffer performance is the ability to suppress changes in $[Na]_i$ during a prolonged period of constant net Na^+ influx. We define the parameter H as the net Na^+ flux remaining with the exchanger operative as a fraction of the net flux without the exchanger. We examine explicitly the dependence of this suppression on various model parameters: M_x, B_t, K_{Ca}, j_0, V_m, $[Na]_o$, and $[Ca]_o$.

We obtain one analytic solution by assuming that the Na/Ca exchanger rate, even if not proportional to $V_m - V_x$, is great enough so that the exchanger never runs far from its equilibrium as defined by Eq. 2. This approximation is valid when the exchanger equilibrium potential for the values of $[Na]_i$ and $[Ca]_f$ that occur during the Na^+ influx deviates by only a few millivolts from the actual value of V_m. This occurs with normal to high physiologic estimates for exchanger flux capacity in our linear model (see above, Fig. 2).

By substituting Eq. 2 into Eq. 3, we derive the equation for $[Ca]_{tot}$ as a function of $[Na]_i$ at exchanger equilibrium. Since B_t is on the order of magnitude mmol/liter or more, and both $[Ca]_f$ and K_{Ca} are order of magnitude μM or less, B_t is from 3 to 5 orders of magnitude greater, and we can readily assume the further approximation that:

$$B_t \simeq B_t + [Ca]_f + K_{Ca} \tag{10}$$

Thus:

$$[Ca]_{tot} = \frac{B_t}{1 + 16\left(\frac{AB_t}{[Na]_i}\right)^3} \tag{11}$$

where we define the dimensionless constant:

$$A = \frac{[Na]_o}{2B_t}\left(\frac{K_{Ca}}{2[Ca]_o}\right)^{1/3} \exp -\left(\frac{V_m F}{3RT}\right) \tag{12}$$

Eq. 11 gives all points in the $[Ca]_{tot}$-$[Na]_i$ plane where, independent of time, the exchanger is in equilibrium (see Fig. 3, *top, solid trace,* which is based on parameter values from Fig. 2).

During the $[Na]^+$ loading phase of the model simulation, the trajectory will be arbitrarily close (by our assumption) to this equilibrium curve, whose slope, $d[Ca]_{tot}/d[Na]_i$, compares the rate at which the exchanger brings in calcium to the net rate at which sodium enters the cell (see Eqs. 4 and 5). We define this net Na^+ influx from all sources as j^*, where $j^* = d[Na]_i/dt$. The difference between j^* and j_0 is the rate at which the exchanger extrudes Na^+, so $-(1/3)\ (j^* - j_0)$ is equal to $d[Ca]_{tot}/dt$. The slope of the equilibrium curve can then be

---

fluxes) to the passive Na^+ leak (j_0). It is plotted on the vertical axis (with values between 0 and 1) and is the minimum value of "$\overline{H}$," the fraction of initial Na^+ influx remaining. On the horizontal axis is the logarithm of the dimensionless variable "B," defined as $(RT/F)\ (M_x/j_0)$ (see Eq. 21). Since RT/F is ~25 mV and j_0 was set to 25 μM/s for the model simulations, B reduces to the parameter value of M_x in units of micromolar per second per millivolt. The traces, from top to bottom, correspond to plots for the following values of the parameter "A" (Appendix): 30, 10, 3, 1, 0.3, 0.1, and 0.03. Values of model parameters used in Fig. 2 correspond to a value of $A \simeq 1.0$. As can be seen in Eq. 12, A varies directly with $K_{Ca}^{1/3}$, but inversely with B_t. The range for $\log[(RT/F)(M_x/j_0)]$ for curves B to F in Fig. 2 is -2.74 to 0.66. The range of values for which there is seen the greatest change in minimum H values is consistent with the results from the simulations in Fig. 2. Simulation results did not significantly change for curves with M_x values smaller than curve B or greater than curve F. Furthermore, the calculated values of minimum H from Eq. 20 (plotted in Fig. 3) deviated by <4% from the values obtained by the simulations displayed in Fig. 2.

expressed as:

$$\frac{d[Ca]_{tot}}{d[Na]_i} = \frac{j_0 - j^*}{3j^*} \tag{13}$$

The ratio of j^* to j_0, or the fraction of j_0 remaining, is defined as "H," which can then be derived as a function of the slope of the equilibrium curve from Eq. 13:

$$H = \frac{j^*}{j_0} = \frac{1}{1 + 3\dfrac{d[Ca]_{tot}}{d[Na]_i}} \tag{14}$$

The maximum suppression of j_0 (i.e., the minimum "H" value) occurs for the maximum value of $d[Ca]_{tot}/d[Na]_i$, i.e., when $d^2[Ca]_{tot}/(d[Na]_i)^2 = 0$. Differentiating Eq. 11 twice with respect to $[Na]_i$ and solving determines a value for $[Na]_i$ equal to $2AB_t$, where A is defined in Eq. 12. Substituting this value for $[Na]_i$ into Eq. 2 above, $[Ca]_f$ at maximum suppression is readily shown to be $K_{Ca}/2$. By substituting $K_{Ca}/2$ for $[Ca]_f$ in Eq. 3, we determine that at maximal suppression the buffer is one-third filled. (For exchangers with a different stoichiometry, the maximal turnover rate will occur at other buffer occupancy values.) To find the value of "H" at maximum suppression, we substitute $2AB_t$ for $[Na]_i$ in the expression for $d[Ca]_{tot}/d[Na]_i$ obtained during the differentiation of Eq. 11. We then substitute this value ($^1/_3A$) into Eq. 14 to yield the minimum value of j^* as a fraction of the original leak (j_0):

$$H = \frac{A}{1 + A} \tag{15}$$

This approximation can also be used to examine the effect of the exchanger on the time constant of the Na^+ decay tails obtained after an abrupt reduction in stimulus rate or reactivation of the pump. Experiments have shown that these tails are generally approximated by a single exponential, and in this analysis we assume such simple kinetics for the Na/K pump. The right side of Eq. 13 now becomes $(j_0 - ([Na]_i/\tau) - j^*)/3j^*$, where τ is the apparent time constant for the Na/K pump acting alone. j^* can then be solved for as above in Eq. 14 to obtain:

$$j^* = \frac{j_0 - ([Na_i]/\tau)}{1 + 3(d[Ca]_{tot}/d[Na]_i)} \tag{16}$$

The apparent time constant when the exchanger is active is obtained by differentiating j^* with respect to $[Na]_i$ in Eq. 16. The maximum increase of τ due to the exchanger is easily obtained by setting $d^2[Ca]_{tot}/(d[Na]_i)^2 = 0$ as above. This simplifies the differentiation and gives an apparent time constant (from Eq. 16) of τ/H.

Thus, if the equilibrium curve of the exchanger-buffer combination is approximately linear over a small range of $[Na]_i$ values or if we are only looking for the maximum effect on the rate constant of decay, the exchanger alters the apparent tail time constant by a multiplicative factor of $(1 + A)/A$ (see Eq. 15) compared with the results for the Na/K pump alone (see also caption of Fig. 2).

Vector Plane Analysis

The second analytic evaluation of H requires that the exchanger rate be proportional to the deviation of the membrane potential from the exchanger equilibrium potential, but relaxes the requirement that this deviation be small. One could conceive that the entire $[Na]_i$-$[Ca]_{tot}$ plane is covered by a vector field, a set of arrows whose components along the $[Na]_i$ and $[Ca]_{tot}$ axes at every point are the values of $d[Na]_i/dt$ and $d[Ca]_{tot}/dt$ from Eqs. 4 and 5 at that

point. It is clear from Eqs. 3 and 6 that this vector field will vary as the parameter B_t, K_{Ca}, V_m, $[Na]_o$, and $[Ca]_o$ vary. A trajectory corresponding to an integration of the model would move from the starting values along a path with direction indicated by the vector field at a rate determined by its local magnitude (Fig. 3, *top*). At a point in the trajectory, the greater the component parallel to the $[Ca]_{tot}$ axis, the more rapidly is the Na-Ca exchanger running, and the greater is the reduction in net Na^+ influx (i.e., $H = j^*/j_0$ is smaller).

The trajectory (*dashed line*) in Fig. 3 (*top*) is an example derived from time course plots *E* of Fig. 2 (*top two panels*), while the solid line represents an equilibrium curve defined by $V_x = V_m$ (see Eq. 6) for the parameter values of the dashed line trajectory. Along all points of the equilibrium curve (*solid line*), the exchanger driving force vanishes and all vectors are horizontal. As one increases the value of M_x, the trajectory becomes arbitrarily close to the equilibrium curve.

At any point, the dot product of the vector and its gradient would be a measure of how the vector field changed as one moved along the trajectory. If this change had the same direction as the original vector, the implication would be that a trajectory at this point would not deviate in direction, i.e., it is at a point of inflection. Since there is only one point of inflection, this point is where the sodium influx rate reaches its minimum. If we call the vector field $\mathbf{C} = [j_0 - 3M_x(V_m - V_x)]\mathbf{i} + [M_x(V_m - V_x)]\mathbf{j}$, and think of it as a function of $[Na]_i$ and $[Ca]_{tot}$, then :

$$\mathbf{C} \times [\mathbf{C} \cdot \mathbf{grad}(\mathbf{C})] = 0 \tag{17}$$

would be an implicit equation in the two variables for the locus of points at which all trajectories on the plane reach their maximal suppression of sodium influx. This equation is just another way of stating that the components of the increment of the vector **C** will be proportional to those of **C** itself at the point.

With a leak that is independent of the intracellular sodium concentration, **C** is the sum of a constant vector with magnitude j_0 in the $[Na]_i$ direction and a vector representing the effects of both the buffer and the Na-Ca exchanger. The latter vector, variable only in amplitude, has a constant direction pointing upwards and to the left at a slope of $-1/3$ due to the exchanger's stoichiometry. Thus, increments of **C** must be parallel to this latter component. They then can never be parallel to **C** itself, which has everywhere the constant leak vector added to the exchanger vector. The above equation can then only be satisfied if there is no increment at all of **C** along some curve, i.e.:

$$\mathbf{C} \cdot \mathbf{grad}(\mathbf{C}) = 0. \tag{18}$$

Using the approximation of Eq. 10, the above equation becomes:

$$0 = 3 - \frac{M_x}{j_0}\left[\frac{[Na]_i B_t + 9[Ca]_{tot}(B_t - [Ca]_{tot})}{[Ca]_{tot}(B_t - [Ca]_{tot})}\right] \cdot \left\{\frac{RT}{F}\ln\left[\frac{(B_t - [Ca]_{tot})[Ca]_0}{[Ca]_{tot}K_{Ca}}\left(\frac{[Na]_i}{[Na]_o}\right)^3\right] - V_m\right\} \tag{19}$$

One can determine the point of minimum sodium influx for all possible trajectories as the extremum of $d[Ca]_{tot}/dt$ along this locus. This is found by solving $\mathbf{grad}(d[Ca]_{tot}/dt) \times \mathbf{grad}\, G = 0$, where G is the right-hand side of Eq. 19, yielding $[Ca]_{tot} = B_t/3$ as before! The lower bound on H, the fraction of j_0 left, can then be obtained as follows. $[Na]_i$ can be written as a function of H by substituting the right-hand side of Eq. 4 for j^* in Eq. 14 and defining V_x by Eq. 6. Using this and the value of $[Ca]_{tot}$, above, in Eq. 19, an implicit equation for the

minimum of H results:

$$H = 1 - \frac{1}{1 + A \exp\left(\frac{1 - H}{9B}\right)} \tag{20}$$

which reduces to Eq. 15 as M_x/j_0 goes to infinity, and where we define a new dimensionless variable:

$$B = \frac{RTM_x}{Fj_0} \tag{21}$$

Of course, this great a suppression of sodium influx could only be attained if the starting initial calcium concentration were sufficiently below that required to fill one-third of the buffer.

We solve this equation numerically and note that $A \simeq 1$ for the following physiologically reasonable estimates used in Fig. 2, i.e., $[Na]_o = 160$ mM, $B_t = 8$ mM, $K_{Ca} = 0.6$ μM, $[Ca]_o = 2$ mM, and $V_m = -50$ mV. Thus for Fig. 2, one would expect H (see Eq. 15) to approach 0.5 for saturating values of M_x/j_0, and predict that $j^* \simeq 0.5\, j_0$, and that the time constant of $[Na]_i$ decay could double, as borne out by the simulation (see also the legend of Fig. 3). Fig. 3 (*bottom*) plots H (the net Na^+ influx as a fraction of j_0) vs. log B for values of A equal to 0.03, 0.1, 0.3, 1, 3, 10, and 30. Both A and B are dimensionless. For the value of j_0 used in Figs. 1 and 2, $B \simeq M_x$ expressed in units of micromoles per second per millivolt.

This work was supported by Program Project Grant Awards HL-30557 and HL-28958, and grants HL-31393 and HL-20558 from National Heart, Lung and Blood Institute.

Original version received 17 September 1987 and accepted version received 2 August 1989.

REFERENCES

Attwell, D., D. Eisner, and I. Cohen. 1979. Voltage clamp and tracer flux data: effects of a restricted extracellular space. *Quarterly Review of Biophysics.* 12:213–261.

Axelson, J., and J. Bridge. 1985. Electrochemical ion gradients and the Na/Ca exchange stoichiometry. *Journal of General Physiology.* 85:471–475.

Baker, P. F., and J. A. Umbach. 1987. Calcium buffering in axons and axoplasm of *Loligo*. *Journal of Physiology.* 383:369–394.

Barry, W. H., C. A. F. Rasmussen, H. Ishida, and J. H. B. Bridge. 1986. External Na independent Ca extrusion in cultured ventricular cells. *Journal of General Physiology.* 88:393–411.

Baumgarten, C. M., and M. Desilets. 1987. Isoproterenol, intracellular Na^+ activity, and the Na/K pump in isolated ventricular myocytes. *In* Recent Studies of Ion Transport and Impulse Propagation in Cardiac Muscle. Wayne Giles, editor. Alan R. Liss Inc., New York. In press.

Blinks, J. R. 1986. Intracellular [Ca] measurements. *In* The Heart and Cardiovascular System. H. Fozzard, E. Haber, R. B. Jennings, A. M. Katz, and H. E. Morgan, editors. Raven Press, New York. 671–701.

Boyett, M. R., G. Hart, and A. J. Levy. 1987. Factors affecting intracellular sodium during repetitive activity in isolated sheep Purkinje fibres. *Journal of Physiology.* 384:405–429.

Bridge, J. H. B. 1986. Relationships between the sarcoplasmic reticulum and sarcoplasmic calcium transport revealed by rapidly cooling rabbit ventricular muscle. *Journal of General Physiology.* 88:437–473.

Bridge, J. H. B., and J. B. Bassingthwaighte. 1983. Uphill sodium transport driven by an inward calcium gradient in heart muscle. *Science.* 219:178–180.

Brinley, F. J., T. Tiffert, and A. Scarpa. 1978. Mitochondria and other calcium buffers of squid axon studied in situ. *Journal of General Physiology.* 72:101–127.

Carafoli, E. 1973. The transport of calcium by mitochondria. Problems and perspectives. *Biochimie.* 55:755–762.

Carafoli, E. 1985. The homeostasis of calcium in heart cells. *Journal of Molecular and Cellular Cardiology.* 17:203–212.

Caroni, P., and E. Carafoli. 1981. The calcium pumping ATPase of heart sarcolemma. Characterization, calmodulin dependence, and partial purification. *Journal of Biological Chemistry.* 256:3263–3270.

Chapman, R. A. 1986. Sodium/calcium exchange and intracellular calcium buffering in ferret myocardium: an ion-selective microelectrode study. *Journal of Physiology.* 373:163–179.

Chapman, R. A., A. Coray, and J. A. S. McGuigan. 1983. Sodium/calcium exchange in mammalian ventricular muscle: a study with sodium-sensitive micro-electrodes. *Journal of Physiology.* 343:253–276.

Chapman, R. A., H. A. Fozzard, I. R. Friedlander, and C. T. January. 1986. Effects of Ca^{++}/Mg^{++} removal on *a*Nai, *a*Ki and tension in cardiac Purkinje fibers. *American Journal of Physiology.* 251:C920–C927.

Cohen, C. J., H. A. Fozzard, and S. S. Sheu. 1982. Increase in intracellular sodium ion activity during stimulation in mammalian cardiac tissue. *Circulation Research.* 50:651–662.

Cohen, I. S., N. B. Daytner, G. A. Gintant, N. K. Mulrine, and P. Pennefather. 1987*a*. Properties of an electrogenic sodium-potassium pump in isolated canine Purkinje myocytes. *Journal of Physiology.* 383:251–267.

Cohen, I. S., R. P. Kline, P. Pennefather, and N. K. Mulrine. 1987*b*. Models of the Na/K pump in cardiac muscle predict the wrong Na^+ activity. *Proceedings of the Royal Society, B* 231:371–382.

Cohen, I. S., and R. P. Kline. 1982. K^+ fluctuations in the extracellular spaces of cardiac muscle: evidence from voltage clamp and K^+-selective extracellular microelectrodes. *Circulation Research.* 50:1–16.

Deitmer, J. W., and D. Ellis. 1978*a*. Changes in the intracellular sodium activity of sheep heart Purkinje fibres produced by calcium and other divalent cations. *Journal of Physiology.* 277:437–453.

Deitmer, J. W., and D. Ellis. 1978*b*. The intracellular sodium activity of cardiac Purkinje fibres during inhibition and re-activation of the Na-K pump. *Journal of Physiology.* 284:241–259.

Deitmer, J. W., and D. Ellis. 1980. Interaction between the regulation of the intracellular pH and sodium activity of sheep cardiac Purkinje fibers. *Journal of Physiology.* 304:471–488.

DiFrancesco, D., and D. Noble. 1985. A model of cardiac electrical activity incorporating ionic pumps and concentration changes. *Philosophical Transactions of the Royal Society of London, B* 307:353–398.

Eisner, D. A., W. J. Lederer, and S. S. Sheu. 1983*a*. The role of intracellular sodium activity in the anti-arrhythmic action of local anaesthetics in sheep Purkinje fibres. *Journal of Physiology.* 340:239–257.

Eisner, D. A., W. J. Lederer, and R. D. Vaughn-Jones. 1983*b*. The control of tonic tension by membrane potential and intracellular sodium activity in the sheep cardiac Purkinje fiber. *Journal of Physiology.* 335:723–743.

Eisner, D. A., W. J. Lederer, and R. D. Vaughn-Jones. 1981*a*. The dependence of sodium pumping and tension on intracellular sodium activity in voltage-clamped sheep Purkinje fibres. *Journal of Physiology.* 317:163–187.

Eisner, D. A., W. J. Lederer, and R. D. Vaughn-Jones. 1981*b*. The effects of rubidium ions and membrane potential on the intracellular sodium activity of sheep Purkinje fibers. *Journal of Physiology.* 317:189–205.

Ellis, D. 1985. Effects of stimulation and diphenylhydantoin on the intracellular sodium activity in Purkinje fibres of sheep heart. *Journal of Physiology.* 362:331–348.

Ellis, D., and K. T. MacLeod. 1985. Sodium-dependent control of intracellular pH in Pukinje fibres of sheep heart. *Journal of Physiology.* 359:81–105.

Ellis, D., and J. Noireaud. 1987. Intracellular pH in sheep Purkinje fibres and ferret papillary muscles during hypoxia and recovery. *Journal of Physiology.* 383:125–141.

Fabiato, A. 1983. Calcium-induced release of calcium from the cardiac sarcoplasmic reticulum. *American Journal of Physiology.* 245:C1–C14.

Falk, R., and I. S. Cohen. 1984. Membrane current following activity in canine cardiac Purkinje fibers. *Journal of General Physiology.* 83:771–799.

Fintel, M. C., and G. A. Langer. 1986. Compartmentation of cellular calcium in rabbit ventricle dependent upon its transsarcolemmal route. *Journal of Molecular and Cellular Cardiology.* 18:1277–1286.

Fischmeister, R., and M. Horackova. 1983. Variation of intracellular Ca^{++} following Ca^{++} current in heart: a theoretical study of ionic diffusion inside a cylindrical cell. *Biophysical Journal.* 41:341–348.

Fry, C. H., D. P. Harding, and J. P. Mounsey. 1987. The effects of cyanide on intracellular ionic exchange in ferret and rat ventricular myocardium. *Proceedings of the Royal Society of London, B.* 230:53–75.

Fry, C. H., T. Powell, V. W. Twist, and J. P. T. Ward. 1984*a*. Net calcium exchange in adult rat ventricular myocytes: an assessment of mitochondrial calcium accumulating capacity. *Proceedings of the Royal Society of London, B.* 223:223–238.

Fry, C. H., T. Powell, V. W. Twist, and J. P. T. Ward. 1984*b*. The effects of sodium, hydrogen, and magnesium ions on mitochondrial calcium sequestration in adult rat ventricular myocytes. *Proceedings of the Royal Society of London, B.* 223:239–254.

Gadsby, D. C., and P. F. Cranefield. 1979. Electrogenic sodium extrusion in cardiac Purkinje fibers. *Journal of General Physiology.* 73:819–837.

Glitsch, H., and H. Pusch. 1984. On the temperature dependence of the Na pump in sheep Purkinje fibres. *Pflügers Archiv.* 402:109–115.

Greenwalt, J. W., C. S. Rossi, and A. L. Lehninger. 1964. Effect of active accumulation of calcium and phosphate ions on the structure of rat liver mitochondria. *Journal of Cell Biology.* 23:21–38.

Hasin, Y., and W. H. Barry. 1984. Myocardial metabolic inhibition and membrane potential, contraction and potassium uptake. *American Journal of Physiology.* 247:H322–H329.

Hodgkin. A. L., P. A. McNaughton, and B. J. Nunn. 1987. Measurement of sodium-calcium exchange in salamander rods. *Journal of Physiology.* 391:347–370.

Jacob, R., D. Piwnica-Worms, C. R. Horres, and M. Lieberman. 1984. Theoretical effects of transmembrane electroneutral exchange on membrane potential. *Journal of General Physiology.* 83:47–56.

January, C. T., and H. A. Fozzard. 1984. The effects of membrane potential, extracellular potassium and tetrodotoxin on the intracellular sodium ion activity of sheep cardiac muscle. *Circulation Research.* 54:652–665.

Johnson, E. A., and J. M. Kootsey. 1985. A minimum mechanism for Na-Ca exchange: net and unidirectional Ca^{++} fluxes as functions of ion composition and membrane potential. *Journal of Membrane Biology.* 86:167–187.

Kass, I. S., and P. Lipton. 1986. Calcium and long-term transmission damage following anoxia in dentate gyrus and CA1 regions of the rat hippocampal slice. *Journal of Physiology.* 378:313–334.

Kumura, J., S. Miyamae, and A. Noma. 1987. Identification of sodium-calcium exchange current in single ventricular cells of guinea-pig. *Journal of Physiology.* 384:199–222.

Kline, R. P., and J. Kupersmith. 1982. Effects of extracellular potassium accumulation and sodium pump activation on automatic canine Purkinje fibres. *Journal of Physiology.* 324:507–533.

Kootsey, J. M., E. A. Johnson, and J. B. Chapman. 1980. Electrochemical inhomogeneity in ungulate Purkinje fibers: model of electrogenic transport and diffusion in clefts. *In* Advances in Physiological Science Vol. 8, Cardiovascular Physiology: Heart, Peripheral Circulation and Methodology. A. G. B. Kovach, E. Menos, and G. Rubanyi, editors. *Proceedings of the International Congress of Physiological Science.* 83–92.

Langer, G. A. 1964. Kinetic studies of calcium distribution in ventricular muscle of the dog. *Circulation Research.* 15:393–405.

Langer, G. A. 1974. Calcium in mammalian myocardium. *Circulation Research Supplement* III. 34,35:91–97.

Levis, R. A., R. T. Mathias, and R. S. Eisenberg. 1983. Electrical properties of sheep Purkinje strands: electrical and chemical potentials in the clefts. *Biophysical Journal.* 44:225–248.

MacAllister, R. E., D. Noble, and R. W. Tsien. 1975. Reconstruction of the electrical activity of cardiac Purkinje fibers. *Journal of Physiology.* 251:1–59.

Mullins, L. J. 1981. Ion transport in heart. Raven Press, New York. 1–136.

Murphy, E., J. F. Aiton, C. R. Horres, and M. Lieberman. 1983. Calcium elevation in cultured heart cells: its role in cell injury. *American Journal of Physiology.* 245:C316–C321.

Niedergerke, R. 1963. Movements of Ca in beating ventricles of the frog heart. *Journal of Physiology.* 167:551–580.

Philipson, K. D., and R. Ward. 1986. Ca^{++} transport capacity of sarcolemmal Na-Ca exchange. Extrapolation of vesicle data to in vivo conditions. *Journal of Molecular and Cellular Cardiology.* 18:943–951.

Piwnica-Worms, D., R. Jacob, C. R. Horres, and M. Lieberman. 1985. Na/H exchange in cultured chick cardiac cells. *Journal of General Physiology.* 85:43–64.

Robertson, S., J. D. Johnson, and J. D. Potter. 1981. The time-course of Ca^{++} exchange with calmodulin, troponin, parvalbumin, and myosin in response to transient increases in Ca^{++}. *Biophysical Journal.* 34:559–569.

Sanchez-Armass, S., and M. P. Blaustein. 1987. Role of sodium-calcium exchange in regulation of intracellular calcium in nerve terminals. *American Journal of Physiology.* 252:C595–C603.

Schanne, F. A. X., A. B. Kane, E. E. Young, and J. L. Farber. 1979. Calcium dependence of toxic cell death: a final common pathway. *Science.* 206:700–702.

Sheu, S. S., and M. P. Blaustein. 1986. Sodium/calcium exchange and regulation of cell calcium and contractility in cardiac muscle, with a note about vascular smooth muscle. *In* The Heart and Cardiovascular System. H. Fozzard, E. Haber, R. B. Jennings, A. M. Katz, and H. E. Morgan, editors. Raven Press, New York. 509–536.

Sheu, S. S., and H. A. Fozzard. 1982. Transmembrane Na^+ and Ca^{++} electrochemical gradients in cardiac muscle and their relationship to force development. *Journal of General Physiology.* 80:325–351.

Sheu, S. S., and H. A. Fozzard. 1985. Na/Ca exchange in the intact cardiac cell. *Journal of General Physiology.* 85:476–478.

Tsien, R. Y., and T. J. Rink. 1980. Neutral carrier ion selective microelectrodes for the measurement of intracellular free calcium. *Biochimica et Biophysica Acta.* 599:623–638.

Vaughan-Jones, R. D., D. A. Eisner, and W. J. Lederer. 1987. Effects of changes of intracellular pH on contraction in sheep cardiac Purkinje fibers. *Journal of General Physiology.* 89:1015–1032.

Walker, J. L. 1986. Intracellular inorganic ions in cardiac tissue. *In* The Heart and Cardiovascular System. H. Fozzard, E. Haber, R. B. Jennings, A. M. Katz, and H. E. Morgan, editors. Raven Press, New York. 561–572.